DOI: 10.1002/ange.200905596

Nanocomposites

Layer-by-Layer Growth of Polymer/Quantum Dot Composite Multilayers by Nucleophilic Substitution in Organic Media**

*Bokyoung Lee, Younghoon Kim, Seryun Lee, Youn Sang Kim, Dayang Wang, and Jinhan Cho**

Layer-by-layer (LbL) self-assembly is a versatile and simple methodology for growing polymer and polymer/inorganic nanoparticle hybrid multilayer thin films with controlled chemical composition and thickness on the nanometer scale.[1] Traditional LbL assembly is carried out in aqueous media and is based on the electrostatic attraction between two oppositely charged materials, such as polycations and polyanions. The recent progress in utilizing hydrogen bonding, click chemistry, disulfide bonding, silanization, esterification, urethane linking, amidation, and so forth, for LbL self-assembly has allowed the growth of multilayer thin films in polar solvents, mainly water and/or alcohols.[2] To our knowledge, LbL self-assembly for functional organic/inorganic nanocomposites has not yet been implemented in nonpolar solvents. Herein we report the first success in using a nucleophilic substitution reaction for LbL self-assembly of organic/inorganic multilayers in nonpolar solvents. Based on a nucleophilic substitution reaction between Br and NH_2, alternating layers of highly hydrophobic CdSe@ZnS quantum dots (QDs) capped with 2-bromo-2-methylpropionic acid (BMPA) in toluene or hexane and poly(amidoamine) dendrimer (PAMA) in ethanol were deposited to form QD/PAMA composite multilayer thin films. The resulting thin films exhibited more robust photoluminescence (PL) in air (oxidation) and in the presence of moisture (hydrolysis) than those obtained by electrostatic LbL self-assembly. These results also demonstrate the possibility of LbL growth of patterned films based on nucleophilic substitution with the aid of microcontact printing.

Photoluminescent (and electroluminescent) polymer/QD nanocomposite films are quite important in technical applications and may be used as functional components in electronic devices, such as optical thin films, or for biomedical imaging.[3–8] Nevertheless, there has been limited success in fabricating polymer/QD composite thin films using the LbL self-assembly techniques developed to date, because the PL properties of the embedded QDs are usually poor. Conventional LbL self-assembly techniques are carried out in aqueous or polar media, which means that the QDs, which are produced either directly in aqueous or polar media or obtained through ligand exchange or phase transfer, have poor surface passivation, which makes the PL of the resulting QDs vulnerable either during LbL self-assembly or during the thin film storage. Recent studies have shown that a high packing density of small and hydrophilic thiol ligands reduces the quantum yield of QDs significantly.[9,13] Kotov et al. reported that the PL intensity of composite multilayer thin films of polyelectrolyte and citrate-stabilized CdSe@CdS QDs was increased by 50–500 times after ambient light irradiation for several days owing to surface oxidization on the QDs with ambient oxygen for 3 days,[11] which was accompanied by a notable blue shift in the PL bands with exposure time. To date, the growth of polymer/QD multilayer thin films that preserve the original PL behavior of the QDs is a significant challenge for LbL self-assembly. To circumvent this challenge, we prepared LbL-assembled highly hydrophobic BMPA-stabilized CdSe@ZnS QDs in nonpolar solvents based on nucleophilic substitution of the terminal Br groups of a BMPA coating with the NH_2 groups of PAMA.

CdSe@ZnS QDs consisting of 4 nm CdSe cores and 1 nm ZnS shells stabilized by oleic acid were prepared in hexane or toluene according to a reported method.[12] The original oleic acid stabilizer ligands were replaced with BMPA through ligand exchange, leading to BMPA-stabilized CdSe@ZnS QDs, denoted BMPA-QDs (see the Supporting Information, Figure S1). Ligand exchange reduced the quantum yield of the QDs (relative to coumarin 545) from 59% to 30%. For comparison, the oleic acid stabilizers of the QDs were also replaced with mercapto acetic acid (MAA) through phase transfer (from toluene to aqueous media) to form negatively charged MAA-coated QDs, denoted MAA-QDs (see experimental details in the Supporting Information). In this case, the relative quantum yield of the resulting MAA-QDs at pH 9 was approximately 9%, which shows that using hydrophilic thiol ligands to replace the original hydrophobic ligands caused a dramatic decrease in the PL quantum yield.

[*] B. Lee,[+] Y. Kim,[+] S. Lee, Prof. J. Cho
School of Advanced Materials Engineering
Kookmin University, Seoul 136-702 (Korea)
E-mail: jinhan@kookmin.ac.kr
Prof. Y. S. Kim
Department of Nano Science and Technology
Graduate School of Convergence Science and Technology
Seoul National University, Seoul 151-744 (Korea)
Dr. D. Wang
Max Planck Institute of Colloids and Interfaces
14424 Potsdam (Germany)
[+] These authors contributed equally to this work.

[**] This work was supported by KOSEF grant funded by the Korea government (MEST) (R01-2008-000-10551-0), Korea Research Foundation Grant (2009-0085070, KRF-2008-D00264), "SystemIC2010" project of Korea Ministry of Commerce Industry and Energy, ERC Program of KOSEF grant funded by the Korea Government (MEST) (R11-2005-048-00000-0) and research program 2009 of Kookmin University. Additionally, this work was supported by Research Settlement Fund for the new faculty of SNU and NRF grant (2009-0079463). D.W. is grateful for the Max Planck Society for the financial support.

Supporting information for this article is available on the WWW under http://dx.doi.org/10.1002/anie.200905596.

Dispersions of BMPA-QDs in hexane or toluene and solutions of PAMA in ethanol were used for LbL growth (Figure 1a). The nucleophilic substitution reaction between the Br and NH_2 groups could be implemented within 30 min in non-aqueous media, such as hexane, toluene, and ethanol, under ambient conditions.[13] Nucleophilic substitution between the Br termini of the BMPA-QDs and the NH_2 termini of PAMA was demonstrated by Fourier transform infrared (FTIR) spectroscopy. Compared to those of BMPA-QDs and PAMA, the FTIR spectra of the PAMA/BMPA-QD multilayer thin films showed two noticeable peaks at 1190 and 1100 cm^{-1}, which are the characteristic bands of secondary aliphatic amines formed from a nucleophilic substitution reaction between the primary amines and bromo groups (Figure 1b). Compared to PAMA, the resulting multilayer thin films showed a weak peak at 1550 cm^{-1}, which was assigned to the N–H bending mode of NH_2, further supporting nucleophilic substitution as the driving force to assemble PAMA and BMPA-QDs. As a result, the FTIR spectra demonstrated that the driving force of the association of BMPA-QDs and PAMA is nucleophilic substitution between Br and NH_2, as highlighted in Figure 1a.

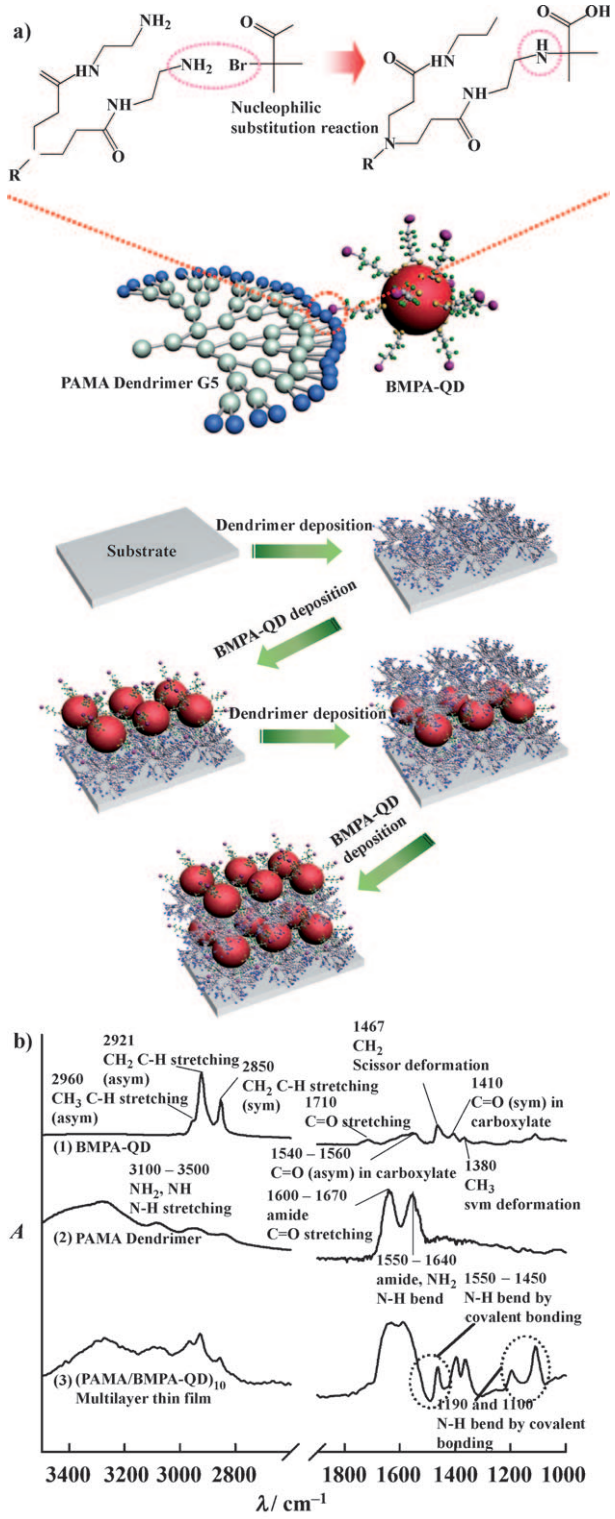

Figure 1. a) Schematic depiction of the buildup of $(PAMA/BMPA\text{-}QD)_n$ multilayer films based on nucleophilic substitution reactions between amino and bromo groups. b) FTIR spectra of 1) BMPA-QDs, 2) PAMA dendrimer, and 3) $(PAMA/BMPA\text{-}QD)_{10}$ multilayers.

The adsorption kinetics of BMPA-QDs on the PAMA layers was examined by quartz crystal microgravimetry (QCM). It followed the typical adsorption isotherm behavior; the amount of BMPA-QDs absorbed onto the PAMA layer reached a plateau within 30 min[14,15] (see the Supporting Information, Figure S2). The frequency change ($-\Delta F$) and mass change (Δm) of BMPA-QDs on the PAMA layer reached a plateau after 30 min absorption: (231 ± 5) Hz and approximately 4081 ng cm^{-2}. These results suggest that during LbL self-assembly, the BMPA-QDs remained stable; otherwise the aggregation of QDs would cause a continuous increase in mass with increasing adsorption time. Scanning electron microscopy (SEM) and atomic force microscopy (AFM) were used to observe the surface morphology of the resulting BMPA-QD coating. The images indicated an increase in QD coverage with increasing adsorption time with no large QD aggregates (Supporting Information, Figure S3).

QCM analysis clearly demonstrated the LbL growth of BMPA-QD/PAMA multilayer thin films based on a NH_2/Br nucleophilic substitution reaction (Figure 2a). The $-\Delta F$ value of each PAMA layer was (9 ± 2) Hz, corresponding to a Δm value of approximately 158 ng cm^{-2}. The $-\Delta F$ of each QD layer was (221 ± 4) Hz, corresponding to a Δm of about 3904 ng cm^{-2}. Considering that the densities of the CdSe core and ZnS shell were approximately 5.81 and 3.89 g cm^{-3}, respectively,[12,15] the number density of QDs in each QD layer was calculated to be approximately 1.3×10^{12} cm^{-2}, corresponding to a packing density of 58%, which is close to the maximum packing density (ca. 64%) for randomly close-packed particle aggregates. This highly dense packing of BMPA-QDs was demonstrated by high-resolution transmission electron microscopy (HR-TEM; Supporting Information, Figure S4). HR-TEM showed no large voids between the QDs. PAMA/MAA-QD multilayer films were also grown in water based on electrostatic attraction, and these films showed a QD packing density much lower than 15% (Supporting Information, Figure S5). Therefore, the high packing density of hydrophobic BMPA-QDs is due to the lack of long-range repulsive forces, that is, electrostatic and

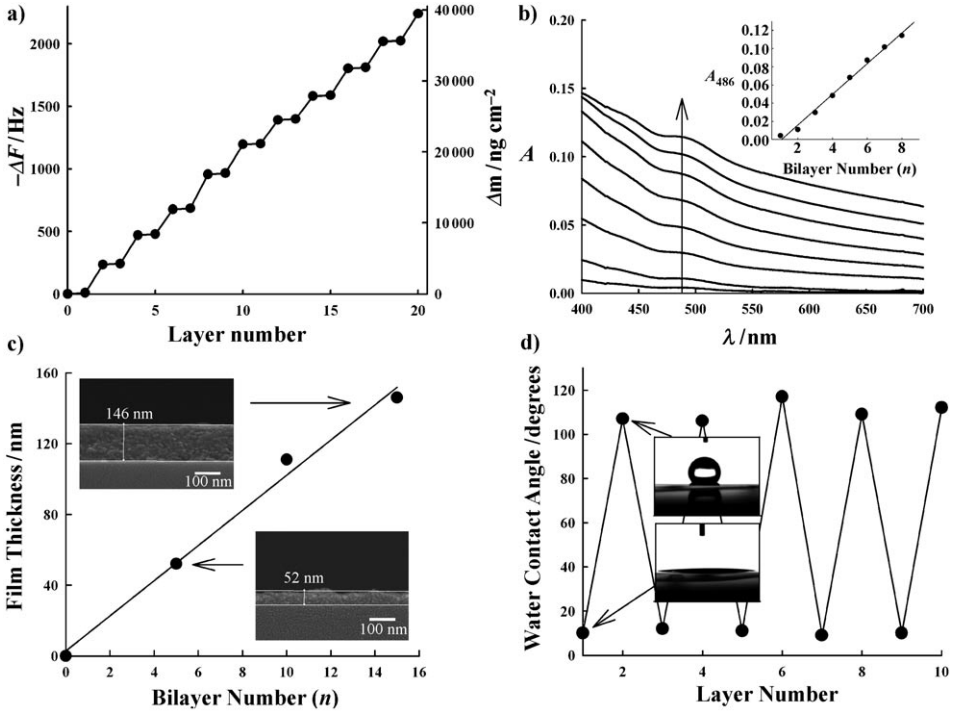

Figure 2. a) QCM data, b) UV/Vis spectra, c) film thickness, and d) the change in surface wettability of $(PAMA/BMPA\text{-}QD)_n$ versus bilayer number *n*. The insets of (b) and (c) show the absorption intensity at 486 nm versus bilayer number and the cross-sectional SEM images, respectively. The inset of (d) displays optical microscopy images of water contact angles. In this case, odd and even numbers indicate PAMA and BMPA-QD layers, respectively.

steric repulsion between the QDs, owing to the small, nonionic BMPA ligand.

Figure 2b shows a linear increase in the absorption intensity of BMPA-QDs with the number of cycles of alternate deposition of BMPA-QDs in toluene and PAMA in ethanol, further demonstrating the LbL growth of BMPA-QD/PAMA multilayers. Figure 2c presents the thickness of BMPA-QD/PAMA multilayer thin films as a function of the number of layers, showing a linear relationship. The average thickness of each layer was approximately 10 nm above the sizes of both CdSe@ZnS QDs and PAMA. As shown in the inset in Figure 2d, the PAMA layer was hydrophilic owing to the terminal NH_2 group, showing a water contact angle of 7°. In contrast, the BMPA-QD layer was hydrophobic owing to the terminal Br and CH_3 groups, giving a water contact angle of about 115°. Therefore, the alternating deposition of BMPA-QDs and PAMA leads to an alternation of the water contact angle on the resulting multilayer films between 7° and 115° (Figure 2d). This result not only demonstrates the LbL growth of BMPA-QD/PAMA multilayer films but also suggests that the surface of the BMPA-QDs remains hydrophobic.

The PL intensity of BMPA-QDs also increased with increasing number of layers, while the PL maximum shows a slight red shift (Figure 3a), which is believed to be due to the energy transfer of smaller QDs to larger ones in the BMPA-QDs ensembles.[16] For comparison, two different CdSe@ZnS QD/PAMA multilayer thin films were prepared by electrostatic attraction in water. The first was derived from mercaptoacetic acid (MAA) as a stabilizer of CdSe@ZnS QDs. The second was derived from block copolymer micelles (BCMs) composed of polystyrene cores, into which the QDs were loaded, and poly(acrylic acid) coronas and was prepared as described in the literature (see experimental details in the Supporting Information).[10,17] The maximum concentration of QDs loaded in the BCMs was $0.57\ mg\,mL^{-1}$, and the quantum yield of the BCM-QDs was approximately 19%. Figure 3b shows that the PL intensity of $(PAMA/BMPA\text{-}QD)_{10}$ thin films was approximately 510 times higher than that of the $(PAMA/MAA\text{-}QD)_{10}$ films and approximately 10 times higher than that of the $(PAMA/BCM\text{-}QD)_{10}$ thin films. The large difference in PL intensity between the three thin films should be determined not only by the relatively high quantum yield of BMPA-QDs and their dense surface coverage per layer but also by the deterioration in the PL behavior of MAA-QDs and BCM-QDs during LbL self-assembly. To gain a better understanding of this phenomenon, the long-term PL stability of the resulting QD/PAMA multilayer films were examined under dark ambient conditions (to avoid photoactivation of the PL behavior of the QDs). Figure 3c shows that the PL intensity of PAMA/BMPA-QD multilayer films was changed slightly after more than one month storage, whereas those of the $(PAMA/MAA\text{-}QD)_n$ and $(PAMA/BCM\text{-}QD)_n$ thin films decreased after one week storage. These results suggest that the hydrophobic character of both BMPA-QDs and their self-assembled layers can prevent PL quenching by hydrolysis and oxidation under ambient conditions and can preserve the original PL behavior of the QDs in the multilayer films.

In conclusion, the nucleophilic substitution reaction between bromo and amino groups was applied successfully to the LbL assembly of highly hydrophobic QDs in nonpolar organic media and polymers in polar organic media into composite multilayer films. This strategy allows the formation of QD/polymer multilayer films with a QD packing density as high as 58% and excellent PL behavior owing to the hydrophobicity of both the QDs and their self-assembly layers. These results should be of significance for technical applications. Similar to the LbL techniques developed to date (i.e., LbL patterning using electrostatic interaction in aqueous

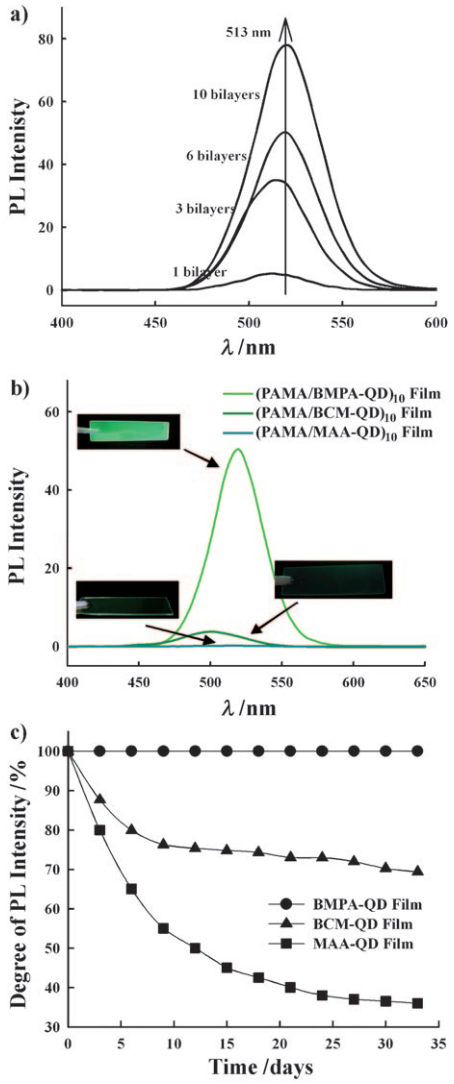

Figure 3. a) The PL spectra of $(PAMA/BMPA\text{-}QD)_n$ multilayers as a function of bilayer number. b) PL spectra and digital camera images of $(PAMA/BMPA\text{-}QD)_{10}$, $(PAMA/BCM\text{-}QD)_{10}$, and $(PAMA/MAA\text{-}QD)_{10}$ multilayers. The concentrations of MAA-QD and BMPA-QD solution were adjusted to 8.57 mg mL^{-1}; the inserted QD concentration of BCM-QD solution was 0.57 mg mL^{-1}. The digital camera images in (b) show the fluorescence of $(PAMA/BMPA\text{-}QD)_{10}$ under irradiation using a 365 nm UV lamp. c) The PL durability of BMPA-QD, BCM-QD, and MAA-QD multilayer films as a function of time. In this case, the solution pH value of PS_{61K}-*b*-PAA_{4K} used as a BCM and MAA was adjusted to be pH 9, and the BMPA-QD with a diameter size of about 5.3 nm exhibited a green color.

media),[11,18] this approach based on nucleophilic substitution also allowed the growth of BMPA-QD/PAMA composite multilayer films on select domains on patterned substrates (see the Supporting Information, Figure S6). This approach opens up a versatile and flexible way of achieving LbL growth of a range of hydrophobic materials (i.e., Fe_2O_3, Pt, Au, or QD nanoparticles) into composite multilayer films in organic media because the process is dependent on the terminal groups of the nanoparticles and polymers rather than on their chemical nature. This process holds immense promise in the fabrication of thin-film electronic devices, such as nonvolatile memory devices.

Experimental Section

Materials: Oleic acid stabilized CdSe@ZnS QDs, 5.3 nm in size, were synthesized as previously reported.[12] For ligand exchange, BMPA (3.34 wt%) was added to a toluene dispersion of the QDs, and the mixture was subsequently heated to 40 °C for 2 h. The removal of excess ligand by centrifugation yielded the BMPA-QDs. The preparation of BCM-QDs and MAA-QDs is shown in the experimental section of the Supporting Information.

Multilayer formation: A dispersion of BMPA-QDs in toluene or hexane and a solution of PAMA in water were prepared at a concentration of 1 mg mL^{-1}. Prior to LbL assembly, the quartz or silicon substrates were cleaned with RCA solution ($H_2O/NH_3/H_2O_2$ 5:1:1 v/v/v). The substrates were first dipped into the PAMA solution for 10 min and were then washed twice with ethanol and dried with a gentle nitrogen stream. The PAMA-coated substrates were dipped into dispersions of BMPA-QDs for 30 min, washed with toluene, and dried with nitrogen. The resulting substrates were dipped into the PAMA solution for 10 min. The above dipping cycles were repeated until the desired number of layers had been obtained.

Measurements: UV/Vis and PL spectra were measured using a Perkin–Elmer Lambda 35 UV/Vis spectrometer and a fluorescence spectrometer (Perkin–Elmer LS 55), respectively. The PL spectra of PAMA/BMPA-QD multilayers were measured at excitation wavelengths $\lambda_{ex} \approx 300$ nm. A quartz crystal microbalance (QCM200, SRS) was used to examine the mass of the material deposited after each adsorption step. The resonance frequency of the QCM electrodes was approximately 5 MHz. The adsorbed mass of PAMA and BMPA-QD was calculated from the change in QCM frequency ΔF using the Sauerbrey equation:[19] $\Delta F\,(\mathrm{Hz}) = -56.6\,\Delta m_A$, where Δm_A is the mass change per quartz crystal unit area in μg cm^{-2}. The surface morphology of the $(PAMA/BMPA\text{-}QD)_n$ multilayers adsorbed onto the Si substrates was observed by FE-SEM (model: JSM-7401F, JEOL).

Patterned multilayers: Photo-cross-linkable PS-N_3 (M_n = 28.0 kg mol^{-1}) was synthesized by reversible addition fragmentation transfer (RAFT) polymerization, as reported elsewhere.[12] PS-N_3 (approximately 2 wt% in toluene) was deposited onto silicon substrates by spin-coating at 4000 rpm and subsequent photo-cross-linking through a patterned shadow mask (UV irradiation, λ = 254 nm) for 3 min. Subsequently, using the aforementioned protocol, the PS-N_3-coated silicon substrates were dipped alternately into the PAMA solutions and BMPA-QD dispersions to grow the BMPA-QD/polymer multilayers on the isolated hydrophilic domains.

Received: October 7, 2009
Published online: December 3, 2009

Keywords: multilayers · nucleophilic substitution · patterning · quantum dots · self-assembly

[1] a) G. Decher, *Science* **1997**, *277*, 1232; b) F. Caruso, R. A. Caruso, H. Möhwald, *Science* **1998**, *282*, 1111; c) Y. Ma, W.-F. Dong, M. A. Hempenius, H. Möhwald, G. J. Vancso, *Nat. Mater.* **2006**, *5*, 724; d) P. Podsiadlo, A. K. Kaushik, E. M. Arruda, A. M. Waas, B. S. Shim, J. Xu, H. Nandivada, B. G. Pumplin, J. Lahann, A. Ramamoorthy, N. A. Kotov, *Science* **2007**, *318*, 80.

[2] a) G. K. Such, J. F. Quinn, A. Quinn, E. Tjipto, F. Caruso, *J. Am. Chem. Soc.* **2006**, *128*, 9318; b) J. S. Major, G. J. Blanchard, *Chem. Mater.* **2002**, *14*, 2574; c) K. Wen, R. Maoz, H. Cohen, J. Sagiv, A. Gibaud, A. Desert, B. M. Ocko, *ACS Nano* **2008**, *2*, 579; d) S. B. Roscoe, S. Yitzchaik, A. K. Kakkar, T. J. Marks, *Langmuir* **1996**, *12*, 5338.

[3] a) D. Wang, A. L. Rogach, F. Caruso, *Chem. Mater.* **2003**, *15*, 2724; b) D. Wang, A. L. Rogach, F. Caruso, *Nano Lett.* **2002**, *2*, 857; c) M. Braun, C. Burda, M. A. El-Sayed, *J. Phys. Chem. A* **2001**, *105*, 5548; d) J. Hong, W. K. Bae, H. Lee, S. Oh, K. Char, F. Caruso, J. Cho, *Adv. Mater.* **2007**, *19*, 4364.
[4] Y. H. Niu, A. M. Munro, Y.-J. Cheng, Y. Q. Tian, M. S. Liu, J. L. Zhao, J. A. Bardecker, I. J.-L. Plante, D. S. Ginger, A. K.-Y. Jen, *Adv. Mater.* **2007**, *19*, 3371.
[5] H. Tetsuka, T. Ebina, F. Mizukami, *Adv. Mater.* **2008**, *20*, 3039.
[6] S. Coe, W. K. Woo, M. Bawendi, V. Bulovic, *Nature* **2002**, *420*, 800.
[7] H. Zhang, Z. Cui, Y. Wang, K. Zhang, X. Ji, C. Lu, B. Yang, M. Gao, *Adv. Mater.* **2003**, *15*, 777.
[8] J. Lee, V. C. Sundar, J. R. Heine, M. G. Bawendi, K. F. Jensen, *Adv. Mater.* **2000**, *12*, 1102.
[9] a) I. L. Medintz, H. T. Uyeda, E. R. Goldman, H. Mattoussi, *Nat. Mater.* **2005**, *4*, 435; b) V. R. Hering, G. Gibson, R. I. Schumacher, A. Faljoni-Alario, M. J. Politi, *Bioconjugate Chem.* **2007**, *18*, 1705; c) H. Mattoussi, J. M. Mauro, E. R. Goldman, G. P. Anderson, V. C. Sundar, F. V. Mikulec, M. G. Bawendi, *J. Am. Chem. Soc.* **2000**, *122*, 12142.
[10] J. Hong, W. K. Bae, H. Lee, S. Oh, K. Char, F. Caruso, J. Cho, *Adv. Mater.* **2007**, *19*, 4364.
[11] Y. Wang, Z. Tang, M. A. Correa-Duarte, L. M. Liz-Marzán, N. A. Kotov, *J. Am. Chem. Soc.* **2003**, *125*, 2830.
[12] S. Lee, B. Lee, B. J. Kim, J. Park, M. Yoo, W. K. Bae, K. Char, C. J. Hawker, J. Bang, J. Cho, *J. Am. Chem. Soc.* **2009**, *131*, 2579.
[13] a) K. M. Evans, A. M. Z. Slawin, T. Lebl, D. Philip, N. J. Westwood, *J. Org. Chem.* **2007**, *72*, 3186; b) W. Qiao, J. Zheng, Y. Wang, Y. Zheng, N. Song, X. Wan, Z. Y. Wang, *Org. Lett.* **2008**, *10*, 641.
[14] a) M. Raposo, O. N. Oliveira, *Langmuir* **2002**, *18*, 6866; b) P. Schuetz, F. Caruso, *Chem. Mater.* **2002**, *14*, 4509.
[15] The densities of CdSe and ZnS are about 5.81 and 3.89 $g\,cm^{-3}$, respectively. Therefore, the number density of QDs can be roughly calculated on the basis of the size of CdSe@ZnS (about 5.3 nm) and CdSe core (about 4 nm).
[16] C. R. Kagan, C. B. Murray, M. Nirmal, M. G. Bawendi, *Phys. Rev. Lett.* **1996**, *76*, 1517.
[17] a) Y. Kang, T. A. Taton, *Angew. Chem.* **2005**, *117*, 413; *Angew. Chem. Int. Ed.* **2005**, *44*, 409; b) Y. Kang, K. J. Erickson, T. A. Taton, *J. Am. Chem. Soc.* **2005**, *127*, 13800; c) B.-S. Kim, J.-M. Qiu, J.-P. Wang, T. A. Taton, *Nano Lett.* **2005**, *5*, 1987.
[18] a) I. Lee, M. F. Rubner, P. T. Hammond, *Adv. Mater.* **2002**, *14*, 569; b) S. Jaffar, K. T. Nam, A. Khademhosseini, J. Xing, R. S. Langer, A. M. Belcher, *Nano Lett.* **2004**, *4*, 1421; c) J. Park, I. Kim, H. Shin, M. Jung, I. Lee, Y. S. Kim, J. Bang, F. Caruso, J. Cho, *Adv. Mater.* **2008**, *20*, 1843.
[19] D. Buttry, *Advances in electroanalytical chemistry: Applications of the QCM to electrochemistry*, Marcel Dekker, New York, **1991**.

